

# Encoding Gaussian curvature in glassy and elastomeric liquid crystal polymer networks

Cyrus Mostajeran,<sup>1</sup> Taylor H. Ware,<sup>2,3</sup> and Timothy J. White<sup>2</sup>

<sup>1</sup>*Department of Engineering, University of Cambridge, Cambridge CB2 1PZ, United Kingdom*

<sup>2</sup>*Materials and Manufacturing Directorate, Air Force Research Laboratory,*

*Wright-Patterson Air Force Base, OH 45433, USA*

<sup>3</sup>*Azimuth Corporation, Beavercreek, OH USA*

(Dated: May 19, 2022)

Considerable recent attention has been given to the study of shape formation using modern responsive materials that can be preprogrammed to undergo spatially inhomogeneous local deformations. In particular, nematic liquid crystal polymer networks offer exciting possibilities in this context. In this paper, we discuss the generation of Gaussian curvature in thin nematic sheets using smooth in-plane director fields patterned across the surface. We highlight specific patterns which encode constant Gaussian curvature of prescribed sign and magnitude and present experimental results which appear to support the theoretical predictions. Specifically, we provide experimental evidence for the realization of positive and negative Gaussian curvature in glassy and elastomeric liquid crystal polymer networks through the stimulation of smoothly varying in-plane director fields.

It is well known that inhomogeneous local deformations such as differential growth of thin elastic sheets can lead to the formation of Gaussian curvature and complex shape transitions [1, 2]. Modern responsive materials that can be preprogrammed to undergo prescribed spatially inhomogeneous expansions and contractions in response to external stimuli offer exciting possibilities for the design and production of switchable surfaces for use in a variety of applications [3–6]. Nematic liquid crystalline glasses and elastomers are particularly promising candidates for the responsive material of choice. Liquid crystalline polymer networks consist of long, semiflexible molecular crosslinked chains that possess mesomorphic order. Below certain critical temperatures, the material may possess one-dimensional order where the rod-like molecular elements are locally aligned about the director  $\mathbf{n}$  and the material is said to be in the nematic phase. Liquid crystalline solids experience local deformations in response to light, heat, pH, and other stimuli that change the molecular order. Of particular interest are nematic glasses [7] and elastomers [8], both of which have spontaneous deformation tensors of the form

$$F = (\lambda - \lambda^{-\nu})\mathbf{n} \otimes \mathbf{n} + \lambda^{-\nu} \text{Id}_3, \quad (1)$$

where  $\text{Id}_3$  denotes the identity operator on  $\mathbb{R}^3$ . This describes a local scaling by  $\lambda < 1$  along the director  $\mathbf{n}$  and a scaling by  $\lambda^{-\nu}$  perpendicular to  $\mathbf{n}$ . The parameter  $\nu$  is known as the opto-thermal Poisson ratio and relates the perpendicular and parallel responses. For glasses, we typically have  $\lambda \in (0.96, 1)$  and  $\nu \in (\frac{1}{2}, 2)$  [7, 9], while for elastomers considerably larger strains are possible and  $\nu = \frac{1}{2}$  [8].

In the seminal work [6], Aharoni *et al.* describe the interplay between the nematic director field of a thin elastomeric sheet and the resulting 3D configuration attained upon heating. In particular, they consider the reverse problem of constructing a director field that induces a specified 2D intrinsic geometry. In this paper, we follow

the presentation in [2] and consider 2D in-plane director field patterns on thin nematic sheets. It is assumed that the director field does not vary across the thickness of the sheet so that the same pattern is repeated at each level of thickness. For sufficiently thin sheets, stimulation of the system will result in pure bending of the sheet at no stretch energy cost and one expects an isometric immersion of the prescribed local deformations as determined by the director field pattern.

Let  $(x_1, x_2) \in \omega \subset \mathbb{R}^2$  be Cartesian coordinates parametrising the mid-surface of the initially flat sheet and  $\mathbf{n}(x_1, x_2) = n_1 \hat{\mathbf{e}}^1 + n_2 \hat{\mathbf{e}}^2$  be the director field pattern across the surface, where  $\hat{\mathbf{e}}^1, \hat{\mathbf{e}}^2$  form the standard orthonormal basis of  $\mathbb{R}^2$ . The associated in-plane spontaneous deformation tensor  $F$  has components  $F_{\alpha\beta} = (\lambda - \lambda^{-\nu})n_\alpha n_\beta + \lambda^{-\nu} \delta_{\alpha\beta}$ , where  $\alpha, \beta = 1, 2$ . The resulting 2D metric of the deformed sheet upon stimulation is  $a = F^T F$ , which simplifies to

$$a_{\alpha\beta} = (\lambda^2 - \lambda^{-2\nu})n_\alpha n_\beta + \lambda^{-2\nu} \delta_{\alpha\beta}. \quad (2)$$

We characterise the 2D director field by an angle scalar field  $\psi = \psi(x_1, x_2)$  which specifies the in-plane orientation of the director at each point on the initially flat sheet, so that  $n_1 = \cos \psi$  and  $n_2 = \sin \psi$ . By the *Theorema Egregium* of Gauss, the Gaussian curvature  $K$  of a surface is an intrinsic geometric property that is determined by the first fundamental form  $a_{\alpha\beta}$  of the surface via

$$K = -\frac{1}{a_{11}} \left( \partial_1 \Gamma_{12}^2 - \partial_2 \Gamma_{11}^2 + \Gamma_{12}^1 \Gamma_{11}^2 - \Gamma_{11}^1 \Gamma_{12}^2 + \Gamma_{12}^2 \Gamma_{12}^2 - \Gamma_{11}^2 \Gamma_{22}^2 \right), \quad (3)$$

where  $\Gamma_{\alpha\beta}^\gamma = \frac{1}{2} a^{\gamma\sigma} (\partial_\alpha a_{\sigma\beta} + \partial_\beta a_{\alpha\sigma} - \partial_\sigma a_{\alpha\beta})$  in Einstein notation.

The Gaussian curvature determined by the nematic metric can be expressed in terms of the alignment angle

field  $\psi$  as

$$K = \frac{1}{2} (\lambda^{2\nu} - \lambda^{-2}) [(\partial_2^2 \psi - \partial_1^2 \psi - 4\partial_1 \psi \partial_2 \psi) \sin(2\psi) + 2(\partial_1 \partial_2 \psi + (\partial_2 \psi)^2 - (\partial_1 \psi)^2) \cos(2\psi)]. \quad (4)$$

We note here that if we rotate the director associated with a given pattern by  $\pi/2$  at every point, so that  $\psi \rightarrow \psi + \pi/2$ , then the resulting Gaussian curvature flips sign at every point, since  $\sin 2\psi \rightarrow -\sin 2\psi$  and  $\cos 2\psi \rightarrow -\cos 2\psi$ . That is,

$$K \rightarrow -K \quad \text{as} \quad \psi \rightarrow \psi + \pi/2. \quad (5)$$

We refer to a pair of director field patterns that are related by a  $\pi/2$  radian rotation of the directors as orthogonal duals.

We now restrict our attention to director fields of the form  $\mathbf{n} = \cos \psi(x_2) \hat{\mathbf{e}}^1 + \sin \psi(x_2) \hat{\mathbf{e}}^2$ , whose alignment angle field varies only with respect to one of the coordinates. The Gaussian curvature upon stimulation is  $K = -\frac{1}{2} (\lambda^{-2} - \lambda^{2\nu}) (\psi'' \sin 2\psi + 2\psi'^2 \cos 2\psi)$ . We can rewrite this as

$$\frac{d^2}{dx_2^2} \cos 2\psi = 4C(K), \quad (6)$$

where  $C(K) = K/(\lambda^{-2} - \lambda^{2\nu})$ , and solve for constant  $K > 0$  to find

$$\psi(x_2) = \pm \frac{1}{2} \cos^{-1} \left( c_1 + c_2 x_2 + 2C(K) x_2^2 \right), \quad (7)$$

where  $c_1, c_2$  are constants of integration. This pattern generates constant Gaussian curvature  $K$  wherever it is well-defined. Now consider the particular solution  $\psi(x_2) = \pm \frac{1}{2} \cos^{-1} \left( 2(1 - x_2)^2 - 1 \right)$ , corresponding to  $c_1 = 1, c_2 = -4$  and  $K = \lambda^{-2} - \lambda^{2\nu} > 0$ . This can be rewritten as  $\psi(x_2) = \cos^{-1}(1 - x_2)$ , which describes a well-defined pattern for  $0 \leq x_2 \leq 2$ . The pattern on the square domain  $\omega = [0, 2] \times [0, 2]$  is shown in Fig. 1 a).

By integrating along the director field lines, we notice that the integral curves of this pattern consist of semicircles of unit radius that are shifted along the  $x_1$ -axis. Indeed, this is a specific case of a more general result which we will now discuss. Consider the director field pattern that is generated by translating the semicircle  $\gamma(t) = (R \cos t, R \sin t)$  (for  $-\pi/2 < t < \pi/2$ ) of radius  $R$  along the  $x_1$ -direction. It is natural to change coordinates from the Cartesian  $(x_1, x_2)$  to  $(t, r)$  where  $t$  is the parameter along the curve  $\gamma$  and  $r$  is a new parameter in the direction of translation. That is,  $x_1(t, r) := \gamma_1(t) + r$  and  $x_2(t, r) := \gamma_2(t)$ . The director field  $\mathbf{n} = n_1 \hat{\mathbf{e}}^1 + n_2 \hat{\mathbf{e}}^2$  at each point  $(t, r)$  is given by  $n_1(t) = \frac{\gamma_1'}{\sqrt{\gamma_1'^2 + \gamma_2'^2}}, n_2(t) = \frac{\gamma_2'}{\sqrt{\gamma_1'^2 + \gamma_2'^2}}$ .

The components  $\mathbf{A} = ((\lambda^2 - \lambda^{-2\nu})n_\alpha n_\beta + \lambda^{-2\nu} \delta_{\alpha\beta})$  of the metric in Cartesian coordinates transform according to  $\mathbf{A} \rightarrow \mathbf{J}^T \mathbf{A} \mathbf{J}$ , where  $\mathbf{J}$  is the Jacobian matrix

$$\mathbf{J} = \begin{pmatrix} \partial_t x_1 & \partial_r x_1 \\ \partial_t x_2 & \partial_r x_2 \end{pmatrix}. \quad (8)$$

Now a direct computation using the metric components with respect to the  $(t, r)$  coordinates yields the constant positive Gaussian curvature

$$K = \frac{\lambda^{-2} - \lambda^{2\nu}}{R^2}. \quad (9)$$

In particular, if we seek to encode a particular constant positive Gaussian curvature  $K = K_0 > 0$  across an initially flat sheet, we can do so by encoding the pattern obtained by shifting a semicircle of radius  $R = \frac{1}{\sqrt{K_0}} (\lambda^{-2} - \lambda^{2\nu})^{1/2}$  as shown in Fig. 1 b).

By the observation that the orthogonal dual of a given 2D director field pattern generates the exact opposite Gaussian curvature at every point, we can encode constant negative Gaussian curvature  $K = -K_0$  on a thin nematic sheet by simply using the orthogonal dual of the pattern that encodes positive curvature  $K_0 > 0$ . Returning to the example of Fig. 1 a), where a pattern encoding constant positive curvature  $K = \lambda^{-2} - \lambda^{2\nu}$  was defined on the square domain  $\omega = [0, 2] \times [0, 2]$  by  $\psi(x_2) = \cos^{-1}(1 - x_2)$ , we immediately obtain a pattern on the same domain which encodes constant negative Gaussian curvature  $K = -(\lambda^{-2} - \lambda^{2\nu})$ , by simply taking  $\psi(x_2) = \cos^{-1}(1 - x_2) + \frac{\pi}{2}$ . The resulting pattern is shown in Fig. 1 c). This pattern is generated by shifting a tractrix curve along its axis.

For a surface in  $\mathbb{R}^3$ , the components  $a_{\alpha\beta}$  and  $b_{\alpha\beta}$  of the first and second fundamental forms satisfy a system of algebraic differential equations known as the Gauss-Codazzi-Mainardi equations. Conversely, any pair  $(a, b)$  consisting of a symmetric and positive definite matrix field  $(a_{\alpha\beta})$  and a symmetric matrix field  $(b_{\alpha\beta})$  that satisfy the Gauss-Codazzi-Mainardi equations determines a unique surface up to a rigid transformation in  $\mathbb{R}^3$  [10]. Thus, to determine the equilibrium configuration of the mid-surface of an initially flat nematic sheet upon stimulation, we also need to know the components  $b_{\alpha\beta}$  of the second fundamental form that minimize the bending energy subject to the Gauss-Codazzi-Mainardi constraints.

For a fixed 2D metric, the problem of identifying equilibrium configurations that minimize the bending energy reduces to the problem of minimizing the *Willmore functional*

$$I_W = \int_\omega H^2 dS, \quad (10)$$

where  $H$  is the mean curvature of the deformed surface, among isometric immersions of the given metric [11–13].

For a metric of constant positive Gaussian curvature, it is easy to show that the Willmore functional is minimized precisely for spherical solutions. That is, a flat nematic sheet whose director field encodes constant positive curvature  $K$  is expected to form part of a sphere of radius  $R = 1/\sqrt{K}$  upon stimulation, assuming that the sheet is small enough to exclude the possibility of self-intersection [2].

In the case of a metric of constant negative Gaussian curvature, identifying minimizers of the Willmore

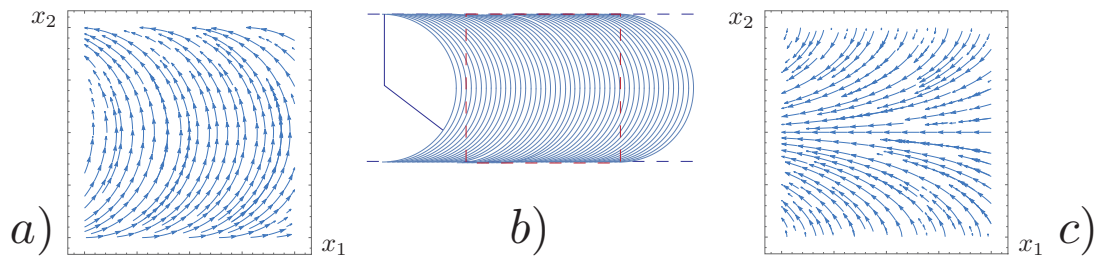


FIG. 1: (Color online) *a*) The director field defined by  $\psi(x_2) = \cos^{-1}(1 - x_2)$  on the square domain  $\omega = [0, 2] \times [0, 2]$ . This pattern generates constant Gaussian curvature  $K = \lambda^{-2} - \lambda^{2\nu} > 0$  upon stimulation. *b*) The nematic pattern obtained by shifting a semicircular arc of radius  $R = \frac{1}{\sqrt{K}} (\lambda^{-2} - \lambda^{2\nu})^{1/2}$  along the  $x_1$ -axis generates constant positive Gaussian curvature  $K > 0$  upon stimulation. *c*) The director field defined by  $\psi(x_2) = \pi/2 + \cos^{-1}(1 - x_2)$  on the square domain  $\omega = [0, 2] \times [0, 2]$ . This pattern generates constant negative Gaussian curvature  $K = -(\lambda^{-2} - \lambda^{2\nu}) < 0$  upon stimulation.

functional is considerably less straightforward. In [14] it is shown that for a hyperbolic elastic disc that has already undergone local deformations, surfaces that are geodesic discs lying on hyperboloids of revolution of constant Gaussian curvature are minimizers of the Willmore functional among *smooth* immersions of the metric. These solutions will appear as saddle shapes in experiments and are expected to be energetically favorable for sufficiently small discs. However, it has been shown numerically that certain non-smooth wavy surfaces formed as odd periodic extensions of subsets of so-called Amsler surfaces are energetically more favorable than the smooth saddle shapes that correspond to discs lying on hyperboloids of revolution when the radius of the hyperbolic disc is sufficiently large [15]. We synthesize liquid crystal polymer films with spatially programmed directors in order to realize shape-changing surfaces that exhibit these phenomena.

The director profile in nematic liquid crystal polymer networks can be programmed through a variety of methods, including mechanical and magnetic fields [16, 17]. Using these methods, however, it is difficult to spatially control the director orientation. Here we use nematic networks whose precursors have been specifically designed to align to treated surfaces. Using this approach low molar mass nematic liquid crystal monomers are filled between two plates separated by a well-defined gap. The treated surfaces, on the interior of the plates, direct the self-assembly of the liquid crystals along a specific orientation through the thickness of the material. By using reactive nematic mesogens, this director orientation can be trapped in an elastic solid. Spatially complex director patterns in liquid crystal cells are prepared using point-by-point photoalignment of an azobenzene dye by irradiation with polarized light [18, 19]. By altering the polarization of the incident light, the in-plane orientation of the director of the liquid crystal can be spatially controlled. The resulting director field is a pixelated approximation of the desired smooth pattern with each pixel measuring  $100 \mu\text{m} \times 100 \mu\text{m}$ .

A number of glassy liquid crystalline polymer networks have been demonstrated to be compatible with surface

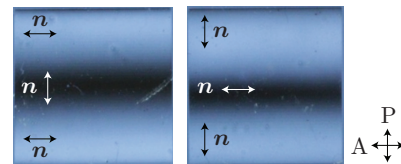


FIG. 2: (Color online) Polarized optical images of the patterned director profiles predicted to generate positive (left) and negative (right) curvature. The patterns are optically equivalent between crossed polarizers. The director orientation at the edges and center of the pattern is indicated with arrows. Each square film has a side length of 10 mm.

alignment techniques. We use one such composition with  $\nu = 0.9$  that is representative of the larger class of nematic liquid crystal glasses that can be aligned using surface alignment techniques [20, 21]. The director patterns depicted in Figures 1.a and 1.c were chosen to assess the viability of generating Gaussian curvature on exposure to stimulus. After fabrication, the liquid crystal network film is flat at  $25^\circ\text{C}$  and retains the expected birefringence of an aligned nematic, as seen in Fig. 2. In the subsequent calculations, we take  $\lambda = 0.97$  as a representative value for  $\lambda$  which is expected to be in the range (0.96, 1) [7, 9].

The thermally-induced shape change of the  $10 \text{ mm} \times 10 \text{ mm}$  square nematic liquid crystal glass in the positive Gaussian curvature case is shown in Fig. 3.a. As predicted, the pattern depicted in Fig. 1.a clearly leads to the formation of positive Gaussian curvature. On removal of the heat, the film returns to a largely flat state. It should be noted that the stimulated sample exhibits a periodic buckling around a pair of opposite edges of the film. This is likely due to the relatively sharp change in director angle with respect to the resolution of the patterning technique near these edges. This buckling highlights the limitation on the curvature that can be achieved in nematic liquid crystal glasses with comparatively small strains for a given patterning resolution.

In order to improve the quality of the surfaces that are formed in stimulated nematic glasses, a discoid subsec-

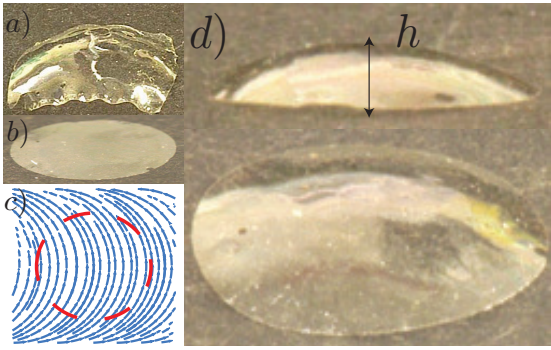


FIG. 3: (Color online) *a)* Positive Gaussian curvature in  $15\ \mu\text{m}$  thick glassy liquid crystal network at  $175^\circ\text{C}$  on a square domain. The periodic buckling near a pair of opposite edges of the film is likely due to the a relatively sharp variation of the director angle for the utilized patterning resolution. *b)* The initially flat configuration of a circular glassy film  $15\ \mu\text{m}$  in thickness and  $7.1\ \text{mm}$  in diameter. *c)* The positive curvature pattern. The dashed circle indicates the boundaries of the circular film. *d)* The formation of positive Gaussian curvature in the actuated state from two distinct viewing angles.

tion of the patterned film was removed and exposed to stimulus, as shown in Fig. 3.d. Note that shape selection of the equilibrium surface of constant positive Gaussian curvature depicted in Fig. 3.d seems to be in remarkable agreement with the predicted solution of a spherical cap. To quantify this agreement, consider the positive curvature pattern of Fig. 3.c on a disc of initial radius  $r_0$ . Since the strains that develop upon stimulating nematic glasses are small, we may assume that the surface of positive Gaussian curvature that is form upon stimulation is approximately a spherical cap; that is, we ignore the variable response on the boundary of the disc and assume that the circular boundary of the disc remains approximately circular. The area of the deformed disc is

$$\mathcal{A} = 2\pi hR \quad (11)$$

where  $R$  is the radius of the resulting spherical cap and  $h$  denotes the height of the spherical cap as shown in Fig. 3.d.  $\mathcal{A}$  is also related to the area  $\mathcal{A}_0$  of the initial disc by

$$\mathcal{A} = \lambda^{1-\nu} \mathcal{A}_0 = \lambda^{1-\nu} \pi r_0^2, \quad (12)$$

since the determinant of the 2D deformation tensor  $F$  is  $\det F = \lambda^{1-\nu}$ . Thus, a measurement of the height  $h$  yields the following estimate for the experimentally realised radius of curvature

$$R_{\text{exp}} = \frac{\lambda^{1-\nu} r_0^2}{2h}, \quad (13)$$

which we can compare with the theoretically predicted radius of curvature given by

$$R = \frac{1}{\sqrt{K}} = \frac{1}{\sqrt{\lambda^{-2} - \lambda^{2\nu}}}. \quad (14)$$

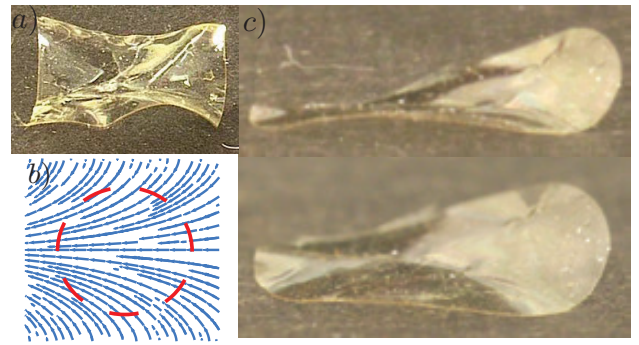


FIG. 4: (Color online) *a)* Negative Gaussian curvature in  $15\ \mu\text{m}$  thick glassy liquid crystal network at  $175^\circ\text{C}$  on a square domain. *b)* The negative curvature pattern obtained as the orthogonal dual director field of the pattern in Fig 3.c. The dashed circle indicates the boundaries of the circular film. *c)* The formation of negative Gaussian curvature in the actuated state of the circular film from two viewing angles.

With an initial diameter of  $d_0 = 2r_0 = 7.1\ \text{mm}$ , an observed height of  $h \approx 2\ \text{mm}$ ,  $\lambda = 0.97$  and  $\nu = 0.9$ , we find that

$$R_{\text{exp}} \approx 3\ \text{mm}, \quad (15)$$

which is consistent with the predicted  $R = 2.9\ \text{mm}$ .

For the negative curvature pattern, the thermally-induced shape change of the  $10\ \text{mm} \times 10\ \text{mm}$  square nematic liquid crystal glass is shown in Fig. 4.a. A discoid film  $7.1\ \text{mm}$  in diameter was removed from the centre of this square film and exposed to stimulus. The resulting equilibrium surface is shown in Fig.4.c and appears largely consistent with a classical hyperboloid saddle. We compare this observation with the results of Gemmer *et al.* in [15]. Consider a disc of radius  $r_0$  encoded with negative Gaussian curvature  $K = -(\lambda^{-2} - \lambda^{2\nu})$ . Since the strains are quite small in nematic glasses (about 1-3 %), we can assume that the radius  $r$  of the hyperbolic disc formed upon stimulation is approximately  $r_0$ . Gemmer's plot in Figure 4 of [15] can be used to determine the energetically favourable hyperbolic surface for the experiment in Fig. 4. The key quantity is

$$\epsilon = r\sqrt{|K|} \approx r_0\sqrt{|K|} = r_0\sqrt{|\lambda^{-2} - \lambda^{2\nu}|}. \quad (16)$$

Note, in particular, that Gemmer identifies a transition at  $\epsilon$  just below 1.5, above which the hyperboloid of revolution saddle becomes less energetically favourable than some periodic Amsler surface. For  $d_0 = 2r_0 = 7.1\ \text{mm}$ ,  $\lambda = 0.97$  and  $\nu = 0.9$ , we have

$$r\sqrt{|K|} \approx 1.2, \quad (17)$$

which falls in the range of  $\epsilon$  where a saddle shape corresponding to a hyperboloid of revolution is energetically favourable. This is consistent with the results observed in Fig. 4.c. Furthermore, for  $\lambda = 0.97$ , a disc of diameter  $10\ \text{mm}$  encoded with negative Gaussian curvature



FIG. 5: (Color online) Side by side comparison of positive (left) and negative (right) Gaussian curvature realization in actuated elastomeric films.

$K = -(\lambda^{-2} - \lambda^{2\nu})$  is expected to form the first of the energetically favourable periodic Amsler surfaces since  $r\sqrt{|K|} \approx 1.7$  in this case [15]. Although this wasn't tried experimentally for a disc, the same pattern on a 10 mm  $\times$  10 mm square generated the surface in Fig. 4.a, which exhibits many of the features of the relevant periodic Amsler solution on a square domain. Due to the tendency for buckling in areas of the film where the director changes rapidly with respect to the resolution of the patterning process, it should be noted that the curvature cannot be increased by simply scaling the pattern to smaller dimensions. Instead a higher patterning resolution or higher strain materials are required.

To facilitate larger curvature realization, we prepare a comparatively high strain surface-alignable liquid crystal elastomer with  $\lambda = 0.65$  [19]. Utilizing the pattern depicted in Fig. 1.a, positive Gaussian curvature is encoded in the elastomeric film. As can be seen in Fig. 5, the film encoded for positive Gaussian curvature forms part of a sphere with a slightly elliptical distortion. It should be noted that the shape transformation occurs despite the tendency of the director within aligned liquid crystal elastomers to be mobile. This “soft elasticity” may be contributing to the elliptical distortion of the film.

Fig. 5 also shows a complexly buckled hyperbolic surface that is formed when an elastomeric disc encoded with negative Gaussian curvature is exposed to stimulus. For smaller diameter films encoded with negative Gaussian curvature, a classic saddle shape can be observed, as shown in Fig. 6. The surface that is formed by the larger radius hyperbolic disc of Fig. 6 can be interpreted as a distorted periodic Amsler surface. Comparatively, these deformations are significantly larger than those observed for the glassy films despite being more than 3 times as thick. Understanding the full spectrum of shape selection for films encoded with negative Gaussian curvature is an area of ongoing consideration.

In summary, our results clearly indicate that Gaussian curvature can be realised in both low-strain, high-

modulus glassy and high-strain, low-modulus elastomeric liquid crystal networks using appropriate smooth in-plane director fields patterned across initially flat films. However, our results suggest that patterned elastomers are not well suited for potential use in devices which may seek to exploit changing metric geometry to achieve repetitive changes in curvature of thin structures. We conjecture that this is mainly due to the mobility of the directors in such material. On the other hand, our preliminary investigations into patterned nematic glasses suggest that glassy liquid crystal polymer networks may indeed be promising candidates for use in applications. In particular, the observed shape transformations were in agreement with the theoretical predictions and the behaviour of the films in response to stimulus was found to be robust and reproducible, unlike the case of elastomeric films. We hope that our results will encourage and stimulate further experimental research in achieving desired shape transitions in glassy liquid crystal polymer networks and further work in assessing the viability of their use for specific applications.

#### ACKNOWLEDGMENTS

CM is supported by the Engineering and Physical Sciences Research Council of the United Kingdom. TJW and THW acknowledge financial support from the Materials and Manufacturing Directorate of the Air Force Research Laboratory and the Air Force Office of Scientific Research. The authors are most grateful to Professor Mark Warner of Cavendish Laboratory for his insightful comments and support.



FIG. 6: (Color online) Comparison of shape selection of discs in the negative Gaussian curvature case depending on the size of the domain. For smaller radii (3.7 mm initial diameter) a saddle shape is formed as expected (right). When the radius of the disc is sufficiently large (7.1 mm initial diameter), considerably more complex surfaces with wavy edges are formed (left).

[1] J. Dervaux and M. Ben Amar, Physical Review Letters **101**, 068101 (2008).  
 [2] C. Mostajeran, Phys. Rev. E **91**, 062405 (2015).

[3] Y. Klein, E. Efrati, and E. Sharon, Science **315**, 1116 (2007).  
 [4] J. Kim, J. A. Hanna, M. Byun, C. D. Santangelo, and

- R. C. Hayward, *Science* **335**, 1201 (2012).
- [5] C. Modes, K. Bhattacharya, and M. Warner, *Proceedings of the Royal Society A: Mathematical, Physical and Engineering Science* **467**, 1121 (2011).
- [6] H. Aharoni, E. Sharon, and R. Kupferman, *Physical review letters* **113**, 257801 (2014).
- [7] C. Van Oosten, K. Harris, C. W. Bastiaansen, and D. Broer, *The European Physical Journal E: Soft Matter and Biological Physics* **23**, 329 (2007).
- [8] M. Warner and E. M. Terentjev, *Liquid crystal elastomers*, Vol. 120 (Oxford University Press, 2003).
- [9] C. D. Modes and M. Warner, *Physical Review E* **84**, 021711 (2011).
- [10] P. G. Ciarlet, *Journal of Elasticity* **78**, 1 (2005).
- [11] M. Lewicka and M. Reza Pakzad, *ESAIM: Control, Optimisation and Calculus of Variations* **17**, 1158 (2011).
- [12] E. Efrati, E. Sharon, and R. Kupferman, *Physical Review E* **83**, 046602 (2011).
- [13] T. J. Willmore, *An introduction to differential geometry* (2012).
- [14] J. A. Gemmer and S. C. Venkataramani, *Physica D: Nonlinear Phenomena* **240**, 1536 (2011).
- [15] J. Gemmer and S. C. Venkataramani, *Soft Matter* **9**, 8151 (2013).
- [16] J. Küpfer and H. Finkelmann, *Die Makromolekulare Chemie, Rapid Communications* **12**, 717 (1991).
- [17] S. Schuhladen, F. Preller, R. Rix, S. Petsch, R. Zentel, and H. Zappe, *Advanced Materials* **26**, 7247 (2014).
- [18] M. E. McConney, A. Martinez, V. P. Tondiglia, K. M. Lee, D. Langley, I. I. Smalyukh, and T. J. White, *Advanced Materials* **25**, 5880 (2013).
- [19] T. H. Ware, M. E. McConney, J. J. Wie, V. P. Tondiglia, and T. J. White, *Science* **347**, 982 (2015).
- [20] J. J. Wie, K. M. Lee, T. H. Ware, and T. J. White, *Macromolecules* **48**, 1087 (2015).
- [21] D. Liu and D. J. Broer, *Langmuir* **30**, 13499 (2014).